



SAKARYA ÜNİVERSİTESİ

FEN BİLİMLERİ ENSTİTÜSÜ DERGİSİ

Sakarya University Journal of Science
SAUJS

ISSN 1301-4048 e-ISSN 2147-835X Period Bimonthly Founded 1997 Publisher Sakarya University
<http://www.saujs.sakarya.edu.tr/>

Title: Using Chemically Unprocessed Orange Peel to Effectively Remove Hg(II) Ions From Aqueous Solutions: Equivalent, Thermodynamic, And Kinetic Investigations

Authors: Yalçın ALTUNKAYNAK

Received: 2022-03-02 00:00:00

Accepted: 2022-12-30 00:00:00

Article Type: Research Article

Volume: 27

Issue: 1

Month: February

Year: 2023

Pages: 189-203

How to cite

Yalçın ALTUNKAYNAK; (2023), Using Chemically Unprocessed Orange Peel to Effectively Remove Hg(II) Ions From Aqueous Solutions: Equivalent, Thermodynamic, And Kinetic Investigations. Sakarya University Journal of Science, 27(1), 189-203, DOI: 10.16984/saufenbilder.1081514

Access link

<https://dergipark.org.tr/en/pub/saufenbilder/issue/75859/1081514>

New submission to SAUJS

<http://dergipark.gov.tr/journal/1115/submission/start>

Using Chemically Unprocessed Orange Peel to Effectively Remove Hg(II) Ions From Aqueous Solutions: Equivalent, Thermodynamic, And Kinetic Investigations

Yalçın ALTUNKAYNAK *¹ 

Abstract

This study looks at the capacity of raw orange peel (ROP) to adsorb Hg²⁺ ions from aqueous solutions. According to the results obtained, it is aimed at using ROPs more efficiently by recycling them. In this way, the usability of both ROP and other agricultural wastes in adsorption processes can be investigated. The effects of many variables on adsorption efficiency were investigated in the study, including initial metal ion concentration (MIC), contact time (CT), and pH. Under optimal operating conditions for Hg²⁺ ion adsorption, CT, solution pH, and initial concentration were determined to be 90 minutes, 3.08, and 180 mg/L, respectively. SEM, Fourier transform infrared spectroscopy (FT-IR), energy dispersion spectroscopy, and Brunauer, Emmett, and Teller (BET) analyses were used to examine the surface features of ROP. The isotherm values were found to be appropriate for the Langmuir isotherm model, indicating chemical absorption and likely process irreversibility. At 318, 308, and 298 K, the capacity of adsorption for the Hg²⁺ ion was calculated to be 66.225, 63.291 and 61.728 mg/g, respectively. The pseudo-second order (PSO), which exhibited the largest regression coefficient and best described the kinetic data for the removal of Hg²⁺ ions, according to thermodynamic studies, it was seen that the adsorption of Hg²⁺ ions on ROP is a natural and endothermic process. ROP, which is abundant throughout the world, can be used effectively in its natural state without any modification or chemical treatment, together with Hg²⁺ adsorption, to remove other heavy metals, dyestuffs, and toxic substances. ROP has been recognized as a potent and promising material for eliminating Hg²⁺ ions from the aquatic environment due to its characteristics such as high adsorption capability, cheap cost, and ease of availability.

Keywords: Langmuir isotherm model, adsorption, orange peel, mercury, second order kinetic model

1. INTRODUCTION

Natural resources are being depleted significantly as a result of factors such as urbanization, population growth,

industrialization, and migration. As a result, the air, land, and water quality continues to deteriorate on a regular basis. Water supplies have been contaminated by industrial processes such as textile, fertilizer

* Corresponding author: altunkaynak4772@gmail.com (Y. ALTUNKAYNAK)

¹ Batman University, Technical Sciences Vocational School

E-mail altunkaynak4772@gmail.com

ORCID: <https://orcid.org/0000-0003-2562-9297>



manufacture, pharmaceutical, paint, and heavy metal. Non-biodegradable heavy metal ions have increased water contamination, posing severe risks to the environment and living beings [1].

Numerous research have been conducted around the world to prevent mercury (Hg^{2+}) pollutions, which have a substantial impact on the ecosystem. Mercury is one of the most poisonous heavy metals, and it is widely released into the environment by industries such as mining, refineries, and coal mining [2]. It causes many major diseases, such as blood, nervous, reproductive system, immune, psychiatric disorders, Alzheimer's disease, cardiovascular difficulties, and so on, due to its high toxicity and significant carcinogenicity [3]. For the reasons described above, the adsorption of Hg^{2+} ions from aqueous solutions has become more important to reduce environmental pollution and improve the quality of life.

Heavy metals and hazardous chemicals can be removed from water, various analytical techniques have been developed. Nano filtration, Membrane separation, ion exchange, adsorption and precipitation are just a few of the techniques available. [4]. While these methods are effective at removing heavy metal ions at high concentrations, they are ineffective at removing metal ions at low concentrations. Adsorption is a more beneficial and practicable way than other methods for eliminating heavy metals at a cheap cost [5]. From aqueous solutions, different adsorbent materials are used by researchers every day to remove heavy metal ions [6]. It is usually preferable to employ a novel adsorbent capable of reducing the concentration of heavy metal ions in aqueous solutions to acceptable levels.

Agricultural and animal wastes have been used as adsorbent in numerous scientific studies [7]. This adsorbent has the benefit of being a low-cost adsorbent with high adsorption capability for inorganic and

organic environmental contaminants. Tetracycline adsorbed carbon, for example, is derived from biogas residue [8]. Tetracycline was adsorbed into the biogas residual at a rate of 58.25 mg/g [9]. The raw orange peel (ROP) utilized in this investigation absorbed Hg^{2+} better than some of the adsorbents described in the scientific literature (Table 3).

Because of their low cost and lack of secondary trash formation, orange peels have recently become popular for heavy metal removal. It is made composed of cellulose, pigments, and hydrocarbons with various hydroxyl functional groups. They also have considerable levels of thiamine, potassium, folacin, calcium, niacin, and magnesium, as well as phytochemicals such limonoids, pectin, hesperidin flavonoid, and polyphenols [10]. Waste orange peels are generally preferred in adsorption experiments because they may be obtained at a very low cost from food processing firms [11]. Due to their low economic worth, orange peels are discarded, polluting the environment. The use of such carbon-rich agricultural products as adsorbent will boost their economic value while reducing their negative environmental effects [12].

The adsorption of Hg^{2+} ions out of aqueous solutions was examined utilizing ROP as an adsorbent in this study manuscript. On metal ion adsorption, the impacts of ROP operational factors including as solution pH, starting MIC, temperature, and CT were studied. The equilibrium isotherm, kinetic, and thermodynamic coefficients were used to compute the adsorption capacity.

2. EXPERIMENTAL

2.1. The Adsorbent Preparation Method

ROP was acquired as an adsorbent in this investigation from Finike oranges purchased from a market in Batman, Turkey. The washed orange peels were dried at room temperature for 7 days. By sifting the crushed ROP, the particle size was lowered to less

than 100 microns. The orange peels were not chemically treated before being used.

2.2. Preparation of Metal Ion Solutions

Mercuric nitrate monohydrate [$\text{Hg}(\text{NO}_3)_2 \cdot 2\text{H}_2\text{O}$] in deionized water was used to make Hg^{2+} ion stock solutions with a concentration of 1000 mg/L for the adsorption investigation. After that, the solutions were produced using the stock solution procedure at reduced concentrations. Each adsorption experiment was carried out with new dilutions. HCl and NaOH solutions were used to prepare solutions at various pH levels. Merck provided the chemicals used in the study.

2.3. Batch Experiments

Mix 25 mL of Hg^{2+} ion solutions with 0.2 g of ROP at concentrations ranging from 100 to 1000 mg/L to examine ROP adsorption kinetics. At 298, 308, and 318 K temperatures, equilibrium was obtained with a continuous stirring speed of 100 rpm. Using the calibration curve technique, Perkin-Elmer Analyst AA2400 atomic absorption spectroscopy (AAS) was used to determine the Hg^{2+} content.

The following equation was used to compute at time t , the quantity of Hg^{2+} ions adsorbed per unit mass.

$$q_t = \frac{C_0 - C_t}{m} V \quad (1)$$

The initial and equilibration metal ion concentrations are supplied by C_0 and C_t (mg/L), respectively, while the amount of Hg^{2+} ion extracted from the adsorbent per mass unit is given by q_t (mg/g).

To explain how concentration affects adsorption, a Hg^{2+} ion stock solution was used to create solutions with concentrations ranging from 100 to 1000 mg/L. To 0.2 g of ROP, a 25 mL sample (100/1000 mg/L) was added. It was shook for 120 minutes at 298, 308, and 318 K. The solutions were then

shaken continuously for 120 minutes. At the end of the shaking period of 120 minutes, it was observed that there was no turbidity in the solution, but a clear yellow color was observed due to the color of the orange peel. This is probably due to the pigments found in the orange peel. This practice also supports similar studies on orange peel in the literature [13]. The quantities of non-adsorbed Hg^{2+} ions were determined using AAS equipment after 120 minutes of shaking. Eq. (1) was used to calculate the amount of metal adsorbed. The initial concentrations that resulted in the greatest amount of adsorption were discovered. As a result of this experiment, the adsorption isotherms for describing equilibration were created

To characterize the CT adsorption results, 0.2 g of ROP was treated with 25 mL of a 600 mg/L Hg^{2+} ion solution. The concentrations of Hg^{2+} in the shaker-mixed samples were measured by AAS at 10-minute intervals from 10 to 120 minutes. The adsorption period at which the Hg^{2+} solution reached saturation was calculated using the data obtained.

PZC refers to the pH biomass surface with a neutral charge PZC was measured in 50 mL of solution with 0.5 g adsorbent (30 °C) at various starting pH values using HCl and NaOH solutions (2.01, 2.94, 3.92, 4.98, 6.08, 6.99, 8.07, 9.02, 10.09, and 11.02). 0.1 mol/L KCl was added to the solution to change its ionic strength. The final pH was taken when the data had reached equilibrium (24 h), allowing for the production of a last pH vs. starting pH plot; and the PZC pH, which matched to the last pH constant value, was defined [13].

To test the effect of pH on removal, 600 mg/L Hg^{2+} ion solutions with pH values ranging from 2 to 6 were created with 0.1 mol/L HCl and 0.1 mol/L NaOH solutions. In a shaker, 25 mL of these solutions were mixed with 0.2 g of ROP and stirred for 120 minutes. An AAS instrument was then used to define the

quantity of metal ions that remained unadsorbed.

2.4. Adsorbent Description

The binding patterns of functional groups found in ROP were investigated using FTIR spectroscopy. Surface features and fundamental analyses were studied using SEM and EDS. At low temperature N_2 sorption, a Brunauer, Emmett, and Teller (BET) analysis was used to compute the specific surface area.

3. RESULTS AND DISCUSSION

3.1. Batch Experiments

3.1.1. The impact of pH on adsorption

PZC is used to evaluate pH in adsorbents when the surface charge transitions from positive to negative. It is defined as the state in which the electrical charge density on a surface is zero. Physical adsorption and ion exchange are linked to ROP sample adsorption capability [14]. Surface groups may gather and keep metal types in aqueous circumstances, where pH variations can impact them, modifying the adsorption process [15]. As a consequence, utilizing PZC definition, a preliminary assessment of the ROP's acid-base behavior was performed. Fig. 1A shows the findings for a 0.1 mol/L KCl solution.

The value of PZC The pH was determined to be 3.66. The residue would have primarily positive surface charges in solutions with a pH less than PZC and mostly negative surface charges in solutions with a pH greater than PZC. PZC was found to be below pH 5.0 in the majority of the residues, with mostly negative surface charges attracting positive metal ions [13].

Studies were carried out at various pH (2–6) ranges to investigate the effect of solution pH on the behavior of Hg^{2+} ions during the adsorption process. Adsorption tests were not carried out at alkaline pH values to avoid the

precipitation of Hg^{2+} ions. The effect of solution pH on Hg^{2+} adsorption is seen in Fig. 1B. At low pH, functional groups such as $-NH-$ and OH are protonated to form $-NH^{2+}-$ and OH^{2+} , respectively, resulting in a decrease in Hg^{2+} binding ability [16]. Furthermore, because of the high electrical interaction between the positively charged face and the Hg^{2+} ion, Hg^{2+} is prevented from reaching the adsorbent. Functional groups are gradually deprotonated as the pH rises. In this circumstance, the adsorbent recovers its binding capacity, and the adsorption capacity increases as the pH of the solution rises. When the pH rises, Hg^{2+} hydrolyzes and changes to $HgOH^+$, which then becomes $Hg(OH)_2$. This mercury inhibits Hg^{2+} ion adsorption. [17].

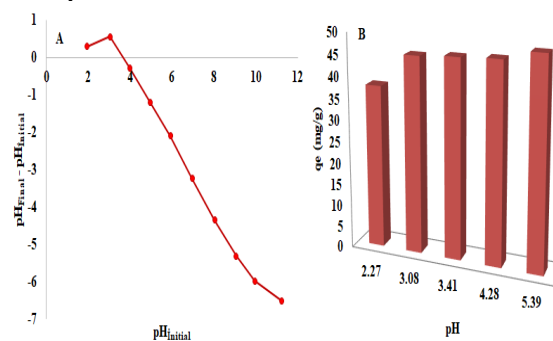


Figure 1 (A) PZC characterization in ROP.

Concentration of KCl: 0.1 mol/L (B) consequence of pH on adsorption of Hg^{2+} using ROP. pH 2.0–6.0, beginning Hg^{2+} ion concentration 600 mg/L

As seen in Figure 1B, the elimination of Hg^{2+} ions is pH dependent. When using 25 mL of Hg^{2+} ion solution with 0.2 g of ROP at a starting concentration of 600 mg/L and pH ranging from 2.0 to 6.0, the elimination capacity varied from 302.7 to 387.4 mg/L in 2 hours. The experiment was continued at pH 3.08, the natural pH solution value, to avoid the precipitation of metal hydroxides in the next phases.

3.1.2. Consequence of CT

The CT of Hg^{2+} ions in the adsorbent solution is a critical feature of the adsorption process. At various temperatures (298, 308 and 318 K) and time intervals, the equilibrium period of a 600 mg/L starting concentration of Hg^{2+}

solution was found to be 90 minutes (10–120 minutes) (Fig. 2). Because of the huge useable surface region, the removal rate of Hg^{2+} ions increased quickly in the first stage. Between the first saturation of the adsorbent surface area and equilibrium, the rate of removal slows [18]. The amounts of Hg^{2+} ions that were retained in equilibrium at starting concentrations of 600 mg/L at working temperatures were computed as 45.237, 42.787, and 41.350 mg/g, respectively, as shown in Fig. 2. The results of this investigation were also utilized to evaluate the adsorption process' kinetics.

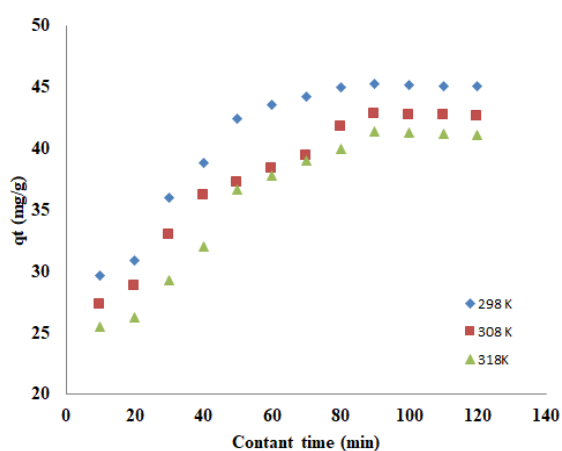


Figure 2 Consequence of CT on Hg^{2+} ion adsorption using ROP. ($V=25$ mL, $C_0=600$ mg/L $m=0.2$ g, pH 3.08)

3.1.3. Adsorption kinetic studies

Kinetic studies were carried out to understand more about the processes of Hg^{2+} ion attachment to ROP and to identify the rate-limiting phase of the process. The CT is a critical factor in the adsorption process. Based on the findings in Fig. 3, the ROP removal capacity was rapidly increased utilizing CT in the early stages. The bulk of Hg^{2+} ions were adsorbed throughout the 90-minute CT. This is because short CTs have a significant number of vacant adsorption sites. As CT increases, target ions fill the empty gaps, and the adsorption process slows down [19]. To gain more thorough data on kinetic

characteristics, nonlinear kinetic modeling was used [20]. The data for removal was analyzed using pseudo-second order (PSO), pseudo-first order (PFO), and Elovich kinetic models. PSO, PFO, and Elovich all have nonlinear kinetic equations (2, 3, 4, respectively) [19]. Weber-Morris kinetic model, on the other hand, might be utilized to explain the film and pore diffusion rates [20]. The abovementioned kinetic model linear form could be demonstrated as in Eq. 5.

$$\ln(q_e - q_t) = \ln q_e - k_1 t \quad (2)$$

$$\frac{t}{q_t} = \frac{t}{q_e} + \frac{1}{k_2 q_e^2} \quad (3)$$

$$q_t = \frac{1}{\beta} \ln(\alpha\beta) + \frac{1}{\beta} \ln t \quad (4)$$

$$q_t = k_d t^{0.5} + C \quad (5)$$

The quantities of adsorbed ions and the equilibrium adsorption capacity at time t are represented by q_t and q_e , respectively, in this equation. The adsorption rate constants for PSO and PFO are k_2 and k_1 , respectively, and is the initial adsorption rate. K_d is the surface coating's adsorption constant, K_d denotes the reaction rate constant, and C denotes the intersection point determined by the thickness of the created boundary layer.

Figure 3 and Table 1 illustrate the kinetic values derived from the nonlinear graphs of the models. Table 1 shows that q_e against t value may be calculated for 318, 308, and 298 K, as well as for low R^2 regression coefficients, $q_{\max \text{ exp.}}$, and $q_{\max \text{ calc.}}$. Trials are used to determine a theoretical removal capacity that is near to the value; also, reasonably high R^2 values indicate that the PSO model accurately characterizes the kinetics of Hg^{2+} ion adsorption by ROP. The temperature-dependent increase in estimated k_2 values (298, 308, 318K) demonstrates that the interplays are temperature-dependent.

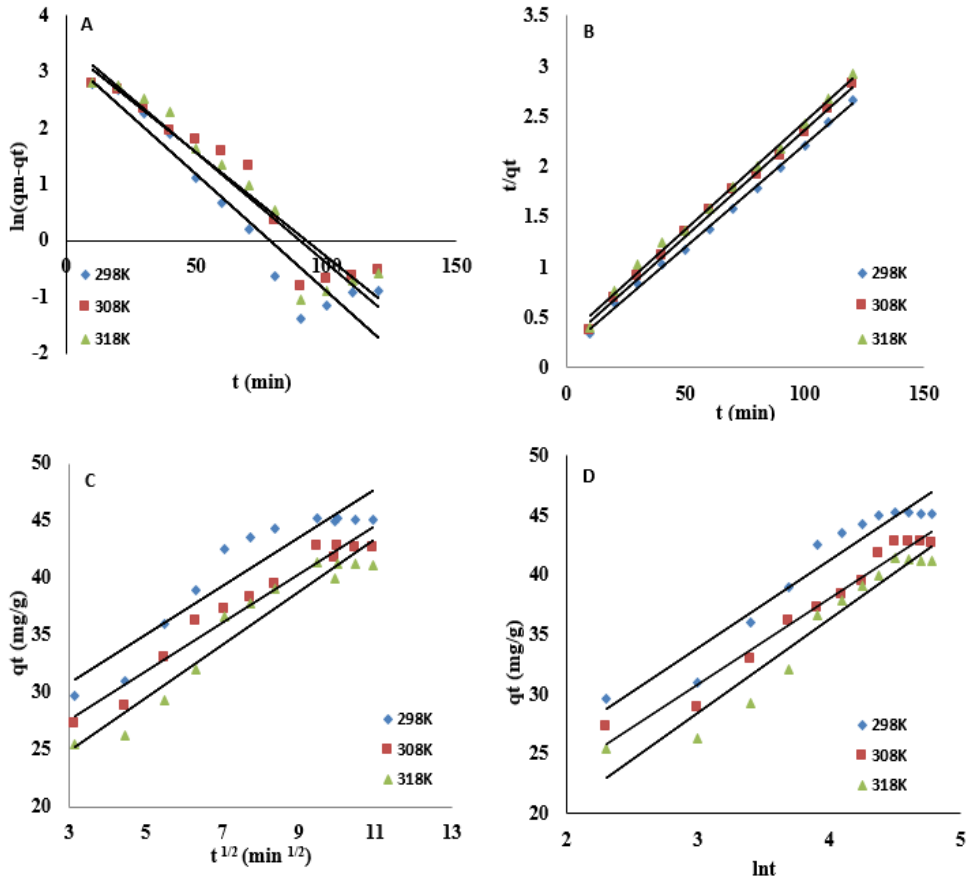


Figure 3 For Hg²⁺ removal through ROP (A) PFO (B) PSO (C) Weber-Morris (D) Elovich model plots

As the temperature rises, the reaction rate constants increase, as seen in Table 1. Using this data, the linearized Arrhenius Eq. (Eq. 6) was used to calculate the activation energy (Ea). Ea was defined to be -14.75 kJ/mol in the adsorption of Hg²⁺ ions by ROP. Ea is less than 4.2 kJ/mol in the presence of weak forces [21]. In activated processes, strong forces give Ea (in chemisorption) ranging from 8.4 to 83.7 kJ/ mol. As a consequence,

the predicted Ea values in this work show that Hg²⁺ ion adsorption through ROP increases chemisorption. The negative Ea value, on the other hand, indicated that a reduction in temperature aided adsorption.

$$\ln k_2 = \ln A - \frac{E_a}{RT} \tag{6}$$

Table 1 Kinetic variables for the removal of Hg²⁺ through ROP at disparate temperatures

Pseudo - First Order					Pseudo - Second Order			
(K)	Line equation	R ²	k ₁	qm	Line equation	R ²	k ₂	qm
298	y=-0.0414x + 3.2389	0.9130	0.0414	25.505	y=0.0215x + 0.2994	0.9945	0.00154	46.511
308	y=-0.0368x + 3.4079	0.9163	0.0368	30.192	y=0.0213x + 0.2435	0.9969	0.00186	46.948
318	y=-0.0392x + 3.5136	0.9148	0.0392	33.568	y=0.0203x + 0.1832	0.9977	0.00224	49.291
Weber- Morris					Elovich			
(K)	Line equation	R ²	K _a	C _b	Line equation	R ²	β	α
298	y=2.1316x+24.331	0.8814	2.1316	24.331	y=7.3458x+11.789	0.9334	0.136	36.596
308	y=2.1232x+21.207	0.9564	2.1232	21.207	y=7.1506x+9.3741	0.9674	0.139	26.688
318	y=2.3175x+17.903	0.9328	2.3175	17.903	y=7.7773x+5.0966	0.9368	0.128	15.044

3.1.4. Adsorption isotherms

As indicated in Fig. 4, the influence of Hg^{2+} ion concentration on adsorption was examined. The removal capacity rose rapidly up to the adsorption saturation limit when the Hg^{2+} ion concentration was raised. As Hg^{2+} ion concentrations increased, the adsorption rate decreased first owing to ROP surface saturation, but finally stabilized after reaching equilibrium. The adsorption isotherm makes it easy to define the adsorbate-adsorbent interaction. It also guarantees that a basic variable process strategy for adsorption goals is in place. Dubinin-Radushkevich, Langmuir, Temkin, and Freundlich isotherms were used to apply data from four nonlinear isotherm models in batch [22, 23].

3.1.4.1. Langmuir isotherm

When a solution's solid face comes into contact with adsorbate particles, it refers to the desorption-adsorption equilibrium. As the adsorbate concentration rises, the adsorption areas gradually get hooked until they reach adsorption saturation, which takes into consideration the greatest monolayer adsorption capacity (q_m). This model implies that homogenous and monolayer adsorption occur in energetically equivalent effective regions. This model is depicted Eq. (7)

$$\frac{C_e}{q_e} = \frac{1}{q_{max} \cdot K_L} + \frac{C_e}{q_{max}} \quad (7)$$

Here, C_e is the MIC at equilibration, q_e denotes the equilibration adsorption capacity, K_L denotes the adsorption constant, and q_m denotes the maximum adsorption capacity. K_L and q_m values were calculated using the nonlinear graphs of q_e and C_e [22].

3.1.4.2. Freundlich isotherm

This model, which accounts for multilayer adsorption and adsorbent surface heterogeneity, is stated as Eq (8).

$$\log q_e = \log K_F + \left(\frac{1}{n}\right) \log C_e \quad (8)$$

In this equation, n and K_F are Freundlich constants that represent density and removal capacity, respectively. These constants' values were obtained using nonlinear plots of experimental data points [22].

3.1.4.3. Dubinin-Radushkevich isotherm

Adsorption may occur on heterogeneous as well as homogeneous surfaces, according to this model, which allows for the separation of physical and chemical adsorption [23]. Eqs. (9 and 10) give an explanation for this model.

$$\ln q_e = \ln q_{max} - K_{DR} \varepsilon^2 \quad (9)$$

$$\varepsilon = RT \ln \left(1 + \frac{1}{C_e}\right) \quad (10)$$

In these equations, the Polanyi potential is represented by ε and the isotherm constant associated with the average adsorption energy is represented by K_{DR} .

3.1.4.4. Temkin isotherm

Because of the interaction between the adsorbate and the adsorbent in this model, the face coverage rises. As a result, the molecules adsorption heat in the layer decreases linearly [24]. The mathematical model in Eq. (11) reopresents these qualities.

$$q_e = \frac{RT}{b_T} + \ln (K_T C_e) \quad (11)$$

Where b_T is the adsorption heat and K_T is the equilibration constant. Plotting q_e versus C_e yielded the b_T and K_T values. Figure 4 shows adsorption isotherm graphs, and Table 2 lists adsorption related variables.

As shown in Fig. 4A, the removal capacity (q_e) rises rapidly at first, then slows as the Hg^{2+} concentration rises, eventually remaining steady after reaching

equilibrium. Figures 4B, 4C, 4D, and 4E provide adsorption equilibration data for the Hg²⁺ ion using Freundlich, Langmuir, Temkin isotherm, and Dubinin-Radushkevich models, respectively. Table 2 shows the variables that were estimated using the provided isotherm models. When Table 2 is studied, it is evident that the Langmuir model, based on R², is the optimal isotherm model for Hg²⁺ ion adsorption. The appropriateness of this

model verifies the process's potential irreversibility and chemisorption. The greatest removal capacity of Hg²⁺ on the ROP was determined as 63.291, 61.728, and 66.225 mg/g at 308, 298 and 318 K, respectively, using Langmuir conditions. This coating has a single layer. The before mentioned characteristic implies that ROP has a high capacity for Hg²⁺ ion adsorption.

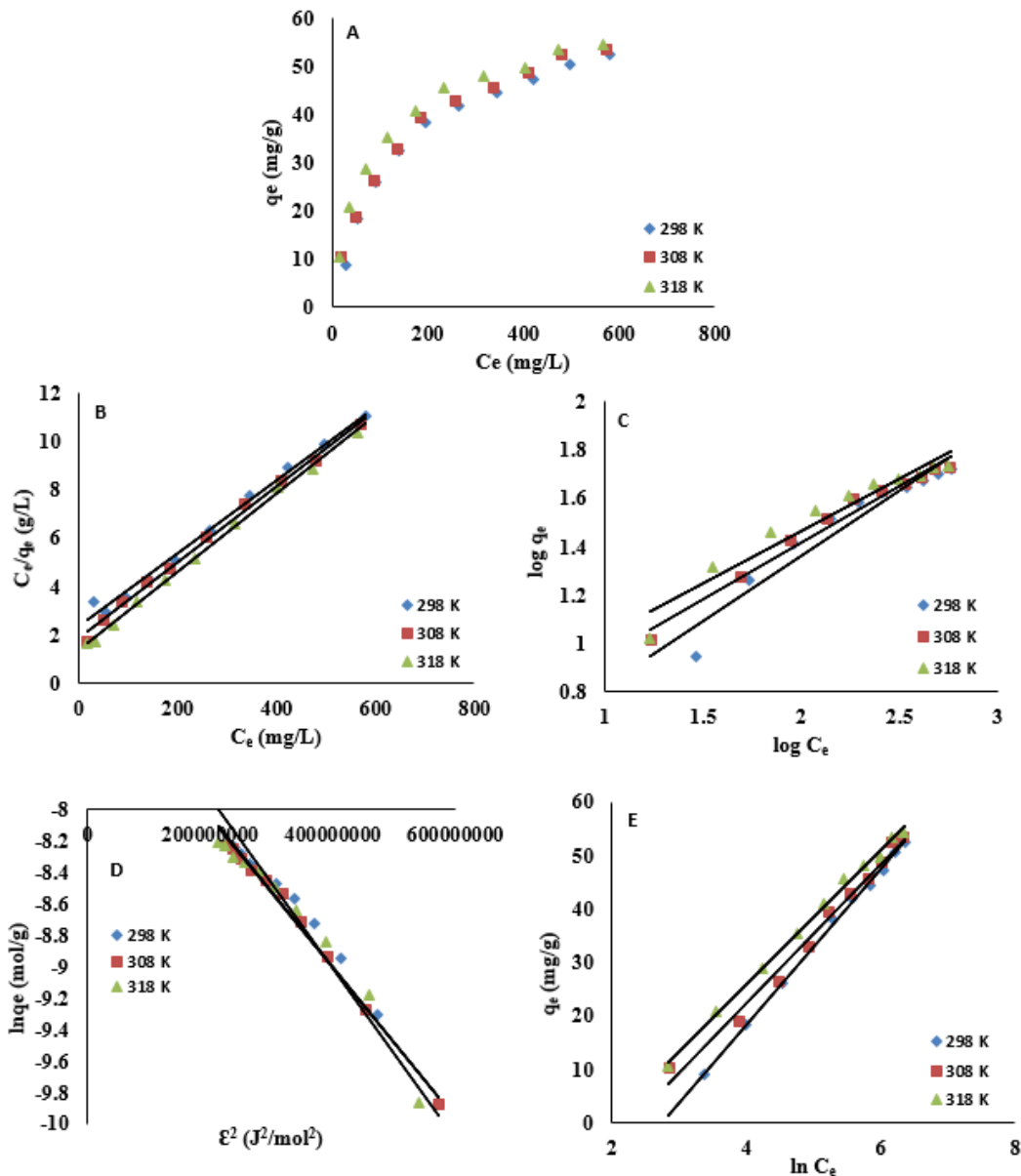


Figure 4 (A Impact of Hg²⁺ ion concentration on adsorption using ROP. (B) Langmuir (C) Freundlich (D) Dubinin-Radushkevich (E) Temkin, isotherm plots

Table 2 Isotherm parameters for removal of Hg²⁺ ions through ROP

Constants		298 K	308 K	318 K
Langmuir	K _L (L/mg)	0.0064	0.0086	0.0121
	q _{max.} (mg/g)	61.728	63.291	66.225
	R ²	0.9934	0.9951	0.9982
Freundlich	n	1.8426	2.1321	2.3068
	K _f	1.8997	3.0164	3.9682
	R ²	0.9288	0.9792	0.9376
Temkin	A _T (L/g)	0.0649	0.1012	0.1429
	b _T (j/mol)	182.284	196.313	197.196
	R ²	0.998	0.9872	0.9974
D-R	K _{D-R}	5.10 ⁻⁹	5.10 ⁻⁹	5.10 ⁻⁹
	E (kj/mol)	10.00	10.00	10.00
	R ²	0.9545	0.9933	0.9642

When analogous investigations for adsorbed Hg²⁺ ions in scholarly articles were analyzed, it was observed that the acquired findings were fairly good. The removal capabilities found in this investigation were compared to those found in previous studies published in the scientific publications indicated in Table 3. ROP adsorption capacity for Hg²⁺ ions were found to be comparable to or superior than values obtained using similar adsorbents. This demonstrates that ROP is a viable material for adsorption procedures.

Table 3 Adsorption capacities of various adsorbents in Hg²⁺ removal were compared

Adsorbent	Adsorption capacity (mg/g)	References
δ-FeOOH	35	[24]
FeMnOOH	12	[25]
Graphene oxide/FeMn composite	33	[26]
MnOX/graphene	2.7	[27]
P-NHT	52.18	[28]
Raw orange peel	61.728 (298K) 63.291 (308K) 66.225 (318K)	This work

3.1.5. Thermodynamic study

Investigating the effect of temperature on the removal of Hg²⁺ ions using ROP will help to

evaluate Enthalpy (ΔH), Entropy (ΔS) and Free energy (ΔG) parameters, which are the basic thermodynamic functions of removal process. The free energy change values (ΔG°) were computed by using Eq. (12).

$$\Delta G^0 = \Delta H^0 - T\Delta S^0 = -RT \ln K_e^0 \quad (12)$$

The equilibration constant K_e^0 , may be computed using Eq.(13) [29]. The abovementioned equation converts the best isotherm model's equilibration constant (K) to a dimensionless thermodynamic equilibration constant.

$$K_e^0 = \frac{(1000KM)[Adsorbate]^0}{\gamma} \quad (13)$$

In this equation, [Adsorbate]₀ stands for adsorbate standard concentration, M represents the molecular weight of the adsorbate, and γ refers to unitary activity coefficient upon the dilution of adsorbate solution.

As regards to Eq. (14), ΔH° and ΔS° are possible to be acquired from the slope and intersection of graph $\ln K_e^0$ versus 1/T.

$$\ln K_e^0 = \frac{\Delta S^0}{R} - \frac{\Delta H^0}{RT} \quad (14)$$

Thermodynamic variables were calculated using reversible methods for Hg²⁺ adsorption through ROP. When looking at the values in Table 4, it is clear that the

distribution constant ($\ln K_d$) is greatly influenced by temperature. What was discovered was that when the temperature climbed, the removal ability for Hg^{2+} ion enhanced. Here, negative ΔG° values indicate that Hg^{2+} ion removal using ROP is a thermodynamically advantageous and natural process. The decline in ΔG° with increasing temperature shows that Hg^{2+} ion removal capacity improves with temperature. ΔH° with positive value of (+16.63 kJ/mol) exhibits that the adsorption of Hg^{2+} through ROP is an endothermic process.

Table 4 ROP was used to calculate Gibbs free energy, enthalpy, and entropy values for Hg^{2+} ions adsorption

Metal	Temperature (K)	$\ln K_d$	ΔG° (kJ/ mol)	ΔH° (kJ/ mol)	ΔS° (J/ mol K)
Hg^{2+}	298	8.240	-20.54	16.63	124.71
	308	8.418	-21.78		
	318	8.667	-23.03		

3.2. Description of Material Pre/Post-Adsorption Experiments

3.2.1. SEM/EDS and definite surface area analysis

The microstructure and surface morphology of the prepared prior to adsorption (Fig. 5A) and post-adsorption (Fig. 5B) are shown in the SEM micrographs. Figure 5A depicts the ROP surface morphology as well-structured layers with no clear orientation due to pectin, cellulose, and hemicellulose producing the orange peel with a limited number of pores. Using BET theory, this morphology yielded $0.756 \text{ m}^2/\text{g}$. On the other hand, The surface morphology of ROP-Hg with very diverse cavities and holes is seen in Figure 5B. The active sites and voids on the ROP surface are also seen to increase after the adsorption process. This explains why novel chemical structures arise on the surface during Hg^{2+} adsorption. The event on the ROP surface can be described as a dissolution-precipitation mechanism that occurs as metal ions adsorb from aqueous solutions [32].

ΔS° positive number indicates that the degree of freedom at the liquid/solid interface grows during the adsorption process [30]. ΔG° low values with positive ΔS° (as observed in Table 4) imply that adsorbate (ROP) properties increase the unpredictability at the liquid-solid interface during Hg^{2+} adsorption. A dissociation mechanism can occur in the adsorbent and adsorbate in this situation, with certain structural changes occurring throughout the removal phase [31].

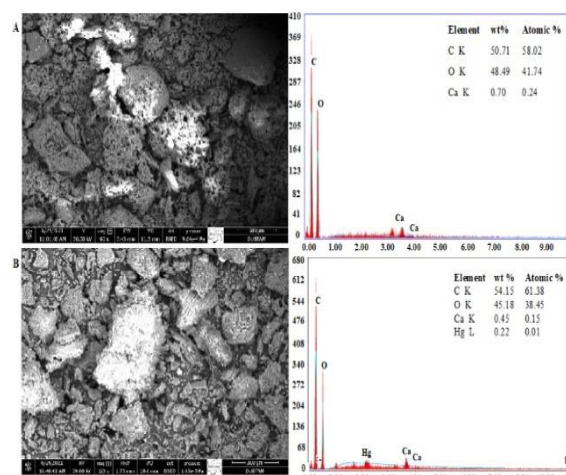


Figure 5 SEM micrograph of ROP and EDS: A) prior to adsorption B) Post-adsorption

3.2.2. FTIR analysis

FT-IR was used to determine the functional groups on the surface of ROP that assist metal ions clinging to the adsorbent or potential removal sites. Figure 6 shows the FT-IR transmission spectra for ROP and ROP-Hg. The intra-intermolecular groups were responsible for the stretching vibration of O-H groups causes widespread extended band absorption at 3291 cm^{-1} . [33]. Aliphatic acid C-H stretching vibrations are responsible for the peak at 2922 cm^{-1} . The peak observed at

1739 cm^{-1} could be due to stretching vibrations for C=O caused by nonionic carboxylic group bonds ($-\text{COOH}$, $-\text{COOCH}_3$). The peaks at 1645 cm^{-1} correspond to lignin skeletal aromatic vibrations of C=C. Finally, the 1014 cm^{-1} peak could represent the primary OH group in lignin or hemicellulose [34]. After the adsorption of Hg^{2+} ions, slight variations in the zenith locations of these functional groups were discovered. For example, while the peak at 3291 cm^{-1} increased to 3325 cm^{-1} , the zenith at 1739 cm^{-1} decreased to 1734 cm^{-1} .

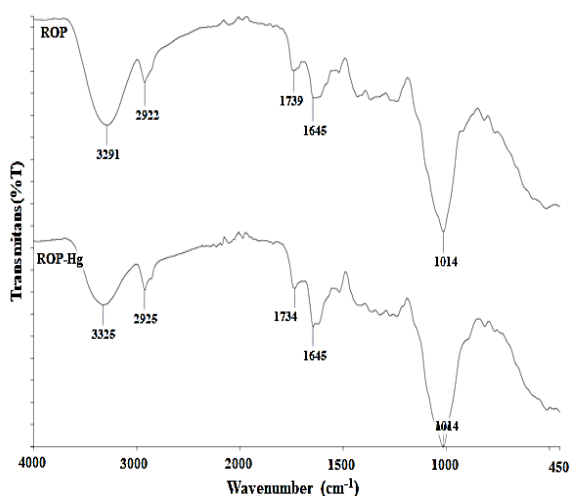


Figure 6 FTIR spectra of ROP and ROP-Hg

3.2.3. Desorption studies

Material regeneration is anticipated to be a critical component in improving separation process costs. The material with high desorption potential indicates that it may be reused in future adsorption procedures. Loading the adsorbent with a certain quantity of metal ions was used to analyze the desorption of mercury from the adsorbent. They were then rinsed with 150 mL of Milli-Q water and dried for a whole day in a 50 °C oven. Following this time, the materials were submerged in a 50 mL solution of 0.1 mol/L HCl to recover the mercury. The adsorption capacity of Hg^{2+} from the aqueous solution was determined at 83.33% using ROP. However, in the desorption study conducted, it was determined that Hg^{2+} was 58.84% desorbed.

Mercury desorbed at low percentage levels even in acidic media. This study shows that ROP strongly adsorbs mercury, which is consistent with the findings of enthalpy and PSO kinetics. This proportion of desorbed ROP was deemed insufficient for future ROP re-use in later adsorption phases.

4. CONCLUSION

ROP was utilized as adsorbent to remove Hg^{2+} ion out of aqueous solutions in this study. When no chemical treatment was applied to the orange peel, it demonstrated outstanding removal performance in the elimination of ions with Hg^{2+} (61.728 (298 K), 63.291 (308 K), and 66.225 (318 K) mg/g. In the natural pH settings of the solutions, the maximum eliminating capability for Hg^{2+} ions was achieved with ROP. pH 3.08 was found to be the value for Hg^{2+} . This system, according to the equilibrium research, followed the Langmuir isotherm model better than other models. The elimination of the Hg^{2+} ion followed the PSO equation, according to kinetic studies. The calculated thermodynamic variables demonstrated the adsorption process's viability and natural character. The enhanced unpredictability of Hg^{2+} at the solid-solution interface was demonstrated by a positive entropy change. The surface area of ROP before adsorption was found to be 0.756 m^2/g by BET analysis. ROP varied considerably before and after adsorption, according to SEM/EDS and FT-IR investigations. The morphological and structural changes that result demonstrate that removal, together with sedimentation, is a key aspect of the process of removing Hg^{2+} from aqueous solution. The reuse of the adsorbent material is very important in terms of cost calculation. In the study conducted to determine the desorption capacity of ROP, 58.84% removal capacity was determined. When the results are analyzed, it is possible to infer that ROP is an effective material to remove Hg^{2+} out of aqueous solutions owing to its inexpensive cost and availability, in addition to its high adsorption capability.

Funding

The author got no financial assistance for this study's research, authorship, or publication.

The Declaration of Conflict of Interest/ Common Interest

The author has disclosed no conflicts of interest or shared interests.

Authors' Contribution

The author made a complete contribution.

The Declaration of Ethics Committee Approval

This study does not require the approval of an ethics committee or any other specific authorisation.

The Declaration of Research and Publication Ethics

“The authors of the paper declare that they comply with the scientific, ethical and quotation rules of SAUJS in all processes of the paper and that they do not make any falsification on the data collected. In addition, they declare that Sakarya University Journal of Science and its editorial board have no responsibility for any ethical violations that may be encountered, and that this study has not been evaluated in any academic publication environment other than Sakarya University Journal of Science.”

REFERENCES

- [1] D. Dai, Z. Li, J. Yang, C. Wang, J. R. Wu, Y. Wang, Y. W. Yang, “Supramolecular assembly-induced emission enhancement for efficient mercury (II) detection and removal,” *Journal of the American Chemical Society*, vol. 141(11), pp. 4756-4763, 2019.
- [2] P. Hadi, M. H. To, C. W. Hui, C. S. K. Lin, G. McKay, “Aqueous mercury adsorption by activated carbons, *Water Research*, vol. 73, pp.37-55, 2015.
- [3] M. A. Rahman, M. S. Rahman, M. J. Uddin, A. N. M. Mamun-Or-Rashid, M. G. Pang, H. Rhim, “Emerging risk of environmental factors: insight mechanisms of Alzheimer’s diseases,” *Environmental Science and Pollution Research*, pp.1-14, 2020.
- [4] A. Benhamou, M. Baudu, Z. Derriche, J. P. Basly, “Aqueous heavy metals removal on amine-functionalized Si-MCM-41 and Si-MCM-48,” *Journal of Hazardous Materials*, vol. 171(1-3), pp. 1001-1008, 2009.
- [5] V. K. Gupta, S. Agarwal, I. Tyagi, D. Pathania, B. S. Rathore, G. Sharma, “Synthesis, characterization and analytical application of cellulose acetate-tin (IV) molybdate nanocomposite ion exchanger: binary separation of heavy metal ions and antimicrobial activity,” *Ionics*, vol. 21(7), pp. 2069-2078, 2015.
- [6] Y. Altunkaynak, “Effectively removing Cu(II) and Ni(II) ions from aqueous solutions using chemically non-processed Midyat stone: equivalent, kinetic and thermodynamic studies,” *Journal of the Iranian Chemical Society*, 2022.
- [7] S. Bhuvaneshwari, H. Hettiarachchi, J. N. Meegoda, “Crop residue burning in India: policy challenges and potential solutions,” *International Journal of Environmental Research and Public Health*, vol. 16(5), pp.832- 851, 2019.
- [8] Q. Cui, W. Zhang, S. Chai, Q. Zuo, K. H. Kim, “The potential of green biochar generated from biogas residue as a heterogeneous persulfate activator and its non-radical degradation pathways: Adsorption and degradation of tetracycline,” *Environmental Research*, vol. 204, pp. 112335, 2022.

- [9] X. Sheng, J. Wang, Q. Cui, W. Zhang, X. Zhu, "A feasible biochar derived from biogas residue and its application in the efficient adsorption of tetracycline from an aqueous solution," *Environmental Research*, vol. 207, pp. 112175, 2022.
- [10] A. Bhatnagar, M. Sillanpää, A. Witek-Krowiak, "Agricultural waste peels as versatile biomass for water purification—A review," *Chemical Engineering Journal*, vol. 270, pp. 244-271, 2015.
- [11] M. Rafatullah, O. Sulaiman, R. Hashim, A. Ahmad, "Adsorption of methylene blue on low-cost adsorbents: a review," *Journal of hazardous materials*, vol. 177 (1-3), pp. 70-80, 2010.
- [12] N. Feng, X. Guo, S. Liang, "Adsorption study of copper (II) by chemically modified orange peel," *Journal of Hazardous Materials*, vol. 164(2-3), pp. 1286-1292, 2009.
- [13] Y. Altunkaynak, M. Canpolat, Ö. Yavuz, "Adsorption of cobalt (II) ions from aqueous solution using orange peel waste: equilibrium, kinetic and thermodynamic studies," *Journal of the Iranian Chemical Society*, pp.1-12, 2021.
- [14] S. Ilhan, A. Cabuk, C. Filik, F. Caliskan, "Effect of pretreatment on biosorption of heavy metals by fungal biomass," *Trakya University Journal of Engineering Sciences*, vol. 5(1), pp. 11-17, 2004.
- [15] Z. Aksu, İ. A. İsoğlu, "Removal of copper (II) ions from aqueous solution by biosorption onto agricultural waste sugar beet pulp," *Process Biochemistry*, vol. 40(9), pp. 3031-3044, 2005.
- [16] W. Tang, J. Gong, L. Wu, Y. Li, M. Zhang, X. Zeng, "DGGE diversity of manganese mine samples and isolation of a *Lysinibacillus* sp. efficient in removal of high Mn (II) concentrations," *Chemosphere*, vol. 165, pp. 277-283, 2016.
- [17] I. Kara, D. Tunc, F. Sayin, S. T. Akar, "Study on the performance of metakaolin based geopolymer for Mn (II) and Co (II) removal," *Applied Clay Science*, vol. 161, pp. 184-193, 2018.
- [18] X. Li, D. Zhang, F. Sheng, H. Qing, "Adsorption characteristics of Copper (II), Zinc (II) and Mercury (II) by four kinds of immobilized fungi residues," *Ecotoxicology and Environmental Safety*, vol. 147, pp. 357-366, 2018.
- [19] Y. A. Neolaka, Y. Lawa, J. N. Naat, A. A. P. Riwu, H. Darmokoesoemo, G. Supriyanto, H. S. Kusuma, "A Cr (VI)-imprinted-poly (4-VP-co-EGDMA) sorbent prepared using precipitation polymerization and its application for selective adsorptive removal and solid phase extraction of Cr (VI) ions from electroplating industrial wastewater," *Reactive and Functional Polymers*, vol. 147, pp. 104451, 2020.
- [20] M. R. Abukhadra, F. M. Dardir, M. Shaban, E. A. Ahmed, M. F. Soliman, "Superior removal of Co^{2+} , Cu^{2+} and Zn^{2+} contaminants from water utilizing spongy Ni/Fe carbonate-fluorapatite; preparation, application and mechanism," *Ecotoxicology and Environmental Safety*, vol. 157, pp. 358-368, 2018.
- [21] M. Kragović, A. Daković, M. Marković, J. Krstić, G. D. Gatta, N. Rotiroti, "Characterization of lead sorption by the natural and Fe (III)-modified zeolite," *Applied Surface Science*, vol. 283, pp. 764-774, 2013.

- [22] E. C. Lima, F. Sher, A. Guleria, M. R. Saeb, I. Anastopoulos, H. N. Tran, A. Hosseini-Bandegharaei, "Is one performing the treatment data of adsorption kinetics correctly?," *Journal of Environmental Chemical Engineering*, vol. 9 (2), pp. 104813, 2021.
- [23] C. Nguyen, D. D. Do, "The Dubinin–Radushkevich equation and the underlying microscopic adsorption description," *Carbon*, vol. 39(9), pp. 1327-1336, 2001.
- [24] L. F. Maia, R. C. Hott, P. C. Ladeira, B. L. Batista, T. G. Andrade, M. S. Santos, J. L. "Rodrigues, Simple synthesis and characterization of l-Cystine functionalized δ -FeOOH for highly efficient Hg (II) removal from contaminated water and mining waste," *Chemosphere*, vol. 215, pp. 422-431, 2019.
- [25] Kokkinos, K. Simeonidis, A. Zouboulis, M. Mitrakas, "Mercury removal from drinking water by single iron and binary iron-manganese oxyhydroxides," *Desalination and Water Treatment*, vol. 54(8), pp. 2082-2090, 2015.
- [26] J. Tang, Y. Huang, Y. Gong, H. Lyu, Q. Wang, J. Ma, "Preparation of a novel graphene oxide/Fe-Mn composite and its application for aqueous Hg (II) removal," *Journal of Hazardous Materials*, vol. 316, pp. 151-158, 2016.
- [27] F. S. Awad, K. M. AbouZeid, W. M. A. El-Maaty, A. M. El-Wakil, M. S. El-Shall, "Efficient removal of heavy metals from polluted water with high selectivity for mercury (II) by 2-imino-4-thiobiuret–partially reduced graphene oxide (IT-PRGO)," *Acs Applied Materials & Interfaces*, vol. 9(39), pp. 34230-34242, 2017.
- [28] S. Das, A. Samanta, G. Gangopadhyay, S. Jana, "Clay-based nanocomposites as recyclable adsorbent toward Hg (II) capture: experimental and theoretical understanding," *ACS omega*, vol. 3(6), pp. 6283-6292, 2018.
- [29] E. C. Lima, A. Hosseini-Bandegharaei, J. C. Moreno-Piraján, I. Anastopoulos, "A critical review of the estimation of the thermodynamic parameters on adsorption equilibria. Wrong use of equilibrium constant in the Van't Hoof equation for calculation of thermodynamic parameters of adsorption," *Journal of Molecular Liquids*, vol. 273, pp. 425-434, 2019.
- [30] V. K. Gupta, "Equilibrium uptake, sorption dynamics, process development, and column operations for the removal of copper and nickel from aqueous solution and wastewater using activated slag, a low-cost adsorbent," *Industrial & Engineering Chemistry Research*, vol. 37(1), pp. 192-202, 1998.
- [31] K. G. Akpomie, F. A. Dawodu, K. O. Adebawal, "Mechanism on the sorption of heavy metals from binary-solution by a low cost montmorillonite and its desorption potential," *Alexandria Engineering Journal*, vol. 54(3), pp. 757-767, 2015.
- [32] G. De Angelis, L. Medeghini, A. M. Conte, S. Mignardi, "Recycling of eggshell waste into low-cost adsorbent for Ni removal from wastewater," *Journal of Cleaner Production*, vol. 164, pp. 1497-1506, 2017.
- [33] C. M. Santos, J. Dweck, R. S. Viotto, A. H. Rosa, L. C. de Moraes, "Application of orange peel waste in the production of solid biofuels and biosorbents," *Bioresource Technology*, vol. 196, pp. 469-479, 2015.

- [34] H. Yang, R. Yan, H. Chen, D. H. Lee, C. Zheng, “Characteristics of hemicellulose, cellulose and lignin pyrolysis,” *Fuel*, vol. 86(12-13), pp. 1781-1788, 2007.